

Assessing the Adversarial Security of Practical Perceptual Hashing Algorithms

Jordan Madden, Moxanki Bhavsar, Lhamo Dorje, and Xiaohua Li, *Senior Member, IEEE*

Abstract—Perceptual hashing algorithms (PHAs) are utilized extensively for identifying illegal online content. Given their crucial role in sensitive applications, understanding their security strengths and weaknesses is critical. This paper compares three major PHAs deployed widely in practice: PhotoDNA, PDQ, and NeuralHash, and assesses their robustness against three typical attacks: normal image editing attacks, malicious adversarial attacks, and hash inversion attacks. Contrary to prevailing studies, this paper reveals that these PHAs exhibit resilience to black-box adversarial attacks when realistic constraints regarding the distortion and query budget are applied, attributed to the unique property of random hash variations. Moreover, this paper illustrates that original images can be reconstructed from the hash bits, raising significant privacy concerns. By comprehensively exposing their security vulnerabilities, this paper contributes to the ongoing efforts aimed at enhancing the security of PHAs for effective deployment.

Index Terms—Perceptual hashing, security, privacy, blackbox adversarial attack, adversarial machine learning

I. INTRODUCTION

Perceptual hashing, also known as robust hashing, is a content fingerprinting technique that generates similar binary hashes for perceptually similar contents and different hashes for different contents [1]. Perceptual hashing is useful in various applications such as content moderation, authentication, and detection. Numerous perceptual hash algorithms (PHAs) have been developed or deployed for practical applications [2]. An early example is the algorithm developed by Google and used on YouTube to identify copyrighted material [3]. Other examples include those used in online image search engines of Google, Microsoft Bing, etc [4].

PHAs have gained critical importance, particularly in responding to the reporting of illicit content. For instance, in cases involving Child Sexual Abuse Media (CSAM), US media service providers are legally obliged to examine suspected illegal content and report it to a “Cyber Tip Line” operated by the National Center for Missing and Exploited Children (NCMEC). Microsoft’s PhotoDNA and Meta’s PDQ have been developed for this purpose [5] [6] [7].

With a growing emphasis on user privacy, technologies like end-to-end encryption have become prevalent. This shift has led to the deployment of PHAs on the client side before data encryption [8]. For example, Apple has proposed to deploy NeuralHash on all its iOS devices [9]. However, deploying PHAs on the client side to scan client data has raised

significant concerns regarding client data privacy, prompting widespread criticism about the robustness and privacy-preserving capabilities of the PHAs [10]. Especially, recent studies have almost unanimously criticized PHAs for their vulnerability to adversarial attacks and the potential leakage of information through hash bits [4] [11] [12].

Given their critical role in sensitive applications, it is imperative to thoroughly understand the security of PHAs. However, even for PHAs that have been widely deployed in the real world, their security remains insufficiently evaluated. Particularly concerning are new PHAs that are hastily deployed without adequate scrutiny. To address this gap, this paper systematically evaluates the adversarial robustness and privacy-preserving capabilities of three widely used PHAs: PhotoDNA, PDQ, and NeuralHash. To support this study, two new efficient attack algorithms are developed.

The major contributions of this paper are as follows.

- A systematic comparison of the security and privacy-preserving capability of three major PHAs against three types of attacks: normal image editing attacks, malicious adversarial attacks, and hash inversion attacks, with the development of a query-efficient adversarial attack algorithm and a data-efficient hash inversion network.
- Demonstrating the robustness of PHAs against malicious adversarial attacks when realistic constraints over distortion and query budget are imposed, contrary to previous studies that neglected such constraints and thus criticized PHAs as being not robust. The robustness is shown to be attributed to the unique property of random hash variations.
- Revealing that the hash bits of all three PHAs leak significant information about the content of the original images, allowing for reliable reconstruction of the original image if sufficient context information is available.

The paper is organized as follows: Section II provides a literature review, Section III formulates the attacks and explains the robustness, Section IV presents the experiment results, and Section V concludes the paper. The source code of the experiments, including the binary executable of the PHAs, can be accessed at <https://github.com/neddami/nhash>.

II. LITERATURE REVIEW

A. Perceptual Hashing Algorithms

Among the vast amount of PHAs [2], this paper considers the following three major ones that have been deployed and used widely in practice:

The authors are with the Department of Electrical and Computer Engineering, Binghamton University, Binghamton, NY 13902, USA. Emails: {jmadden2, mbhavsar2, ldorje1, xli}@binghamton.edu

Manuscript received Mon Day, 2024; revised Mon Day, 2024.

PhotoDNA, released by Microsoft in 2009, has been used by over 70 companies including Cloudflare and Dropbox [6] [13] [14]. To create a hash, PhotoDNA breaks down an image into small pieces, analyzes each piece to extract its unique feature, and converts the features into hash bits. PhotoDNA generates a 144-byte or 1152-bit hash value for each input image.

PDQ, which stands for **P**erceptual algorithm utilising a **D**iscrete Cosine Transform and outputting (amongst others) a **Q**uality metric, was released by Meta in 2019 [7]. Inspired by pHash [15], PDQ uses the discrete cosine transform (DCT) to extract image features and outputs both a 256-bit hash value and a quality factor.

NeuralHash was released by Apple in 2021 with the intent to identify CSAM [9]. An image is first passed through a deep neural network (DNN) to produce a feature embedding. The embedding is then converted to a 96-bit hash. The DNN is trained contrastively to ensure that the cosine similarity between perceptually similar images is high while the similarity of perceptually different images is low.

B. Adversarial Machine Learning

The security of PHAs is commonly studied using the terminologies and algorithms of adversarial machine learning [16]. Specifically, *Adversarial robustness* measures the resilience of the machine learning models to adversarial attacks. *Adversarial attacks* can be classified as untargeted attacks and targeted attacks. In an *untargeted attack*, the objective is to slightly alter the input to prompt the model to produce a completely different output. Conversely, a *targeted attack* aims to slightly modify the input to elicit a specifically designed output.

According to the knowledge that the adversary has about the machine learning model, attacks can be categorized to *whitebox attacks*, where the adversary possesses complete knowledge of the model [16] [17] [18], and *blackbox attacks*, where the adversary only has access to the input and output of the model [19] [20] [21] [22]. In black-box attacks, if the model's outputs are continuous values like logits or probabilities, the attack is referred to as *soft-label attack* [19] [20] [21]. Otherwise, if the model's outputs are solely hard-decision labels, the attack is known as a *hard-label attack* [22].

C. Adversarial Robustness of PHAs

The adversarial robustness of conventional PHAs like pHash [2] was investigated in [23] under the whitebox setting, whereas the robustness under the blackbox setting was explored in [4]. Many of these studies suggested that PHAs were not robust to adversarial attacks.

The adversarial robustness of PhotoDNA, PDQ, and NeuralHash has not been adequately addressed, partly because they are new and partly because their source code is not publicly available. Regarding their robustness to normal image editing, [24] examined PhotoDNA, while [11] investigated PDQ and NeuralHash. Both studies demonstrated that PHAs were robust to certain edits like compression but vulnerable to others like cropping.

As far as we know, [25] was the first to study these PHAs' robustness to adversarial attacks. It studied NeuralHash under the whitebox setting only, and showed that NeuralHash was not robust to whitebox attacks. [26] worked on PDQ and used the linearity of DCT to get adversarial images in a white-box setting. [27] generated adversarial images through linear interpolation between two given images.

Regarding blackbox attacks, [26] studied PDQ and claimed that it was not robust to untargeted blackbox attacks. [28] investigated PhotoDNA and PDQ, concluding that they were not robust to either targeted or untargeted attacks. These two studies closely resemble the current paper, yet this work differs from them in two key aspects. Firstly, previous works computed attack success rates without incorporating limitations on the adversary's tolerance to image quality degradation or query budget. Such constraints are crucial in real-world scenarios. It is trivial that unconstrained blackbox attacks will always be successful, particularly in the untargeted setting. Secondly, none of the prior works conducted a comparative study of the three PHAs, nor did they investigate the challenge of hash inversion.

D. Information Leakage from Hashes

Regarding privacy preservation, upon its release, Microsoft asserted that the hashes generated by PhotoDNA were irreversible and incapable of reconstructing the original images [29]. However, in a blog post [12], it was demonstrated that PhotoDNA hashes leak sufficient information about the original image to allow images to be synthesized from the hashes. To our knowledge, [12] is the sole study on reconstructing the original image from the hash, albeit focusing solely on PhotoDNA that has long hashes. It is unclear if PHAs with short hash suffer from this problem.

Another approach to investigate information leakage is to train a classifier to classify the image objects from the hash. [25] [27] illustrated that NeuralHash hashes indeed revealed information about their source images by enabling the identification of the object's class. Interestingly, these findings contradict those of [30] which examined PhotoDNA hashes and claimed that PhotoDNA was resistant to such classification attacks.

III. ATTACK ALGORITHMS

Consider a perceptual hash system where the service provider scans the client's unencrypted content, extracts a hash for each image using a PHA, compares the hash with a database of known illicit hashes, and raises an alarm or forwards the unencrypted content for further analysis in case of hash match [8]. In this scenario, we consider two adversaries: the client adversary seeking to evade hash matching and the service provider (or some third party) adversary seeking to reconstruct the client's original images from collected hashes.

We evaluate the security of PhotoDNA, PDQ, and NeuralHash against three types of attacks: benign image editing attacks and malicious adversarial blackbox attacks employed by the client adversary, and hash inversion attacks employed by the service provider adversary. Considering the client

adversary, we assess the security of PHAs by measuring the adversary’s attack success rate, where a higher success rate indicates weaker security or robustness. Considering the service provider adversary, security is assessed through image reconstruction quality, where higher quality implies weaker security or privacy.

A. Image Editing Attacks

Assume the original input to the PHA is an image \mathbf{I}_0 , and the true output is an N -bit hash $\mathbf{h}_0 = \mathcal{H}(\mathbf{I}_0)$, where $\mathcal{H}(\cdot)$ denotes the hashing algorithm. The client adversary applies standard image editing operations over \mathbf{I}_0 to obtain an adversarial image \mathbf{I}_{adv} with a new N -bit hash $\mathbf{h}_{\text{adv}} = \mathcal{H}(\mathbf{I}_{\text{adv}})$. A successful attack means \mathbf{h}_{adv} is sufficiently different from \mathbf{h}_0 .

While prior works such as [11] and [24] have investigated image editing attacks on PHAs, a new evaluation is still necessary due to ongoing algorithm updates. Notably, NeuralHash has received at least one update since its first release. This study addresses the gap in knowledge by evaluating the security of the updated algorithms and, more importantly, by providing the first comparison of the three PHAs.

B. Adversarial Blackbox attacks

1) *A Query-efficient Blackbox Attack Algorithm:* This work focuses solely on blackbox, not whitebox, adversarial attacks, reflecting the practical scenario where PHA implementations are proprietary. For some PHAs, details regarding architecture and model weights are not publicly available due to their commercial nature. For instance, Microsoft enforces non-disclosure agreements for PhotoDNA users, and only an emulation is accessible. Similarly, while Ygvar et al. (2021) released weights for the first-generation NeuralHash, Apple has since updated the algorithm, keeping the new model confidential.

Existing blackbox attack algorithms, designed to operate on logits/probabilities or singular class decisions, cannot be directly applied to PHAs because PHAs output a limited number of hash bits, which are neither logits nor class labels. Instead, we propose a joint soft-label hard-label attack (JSHA) algorithm, where a soft-label attack step is applied first and its output is passed as input to a hard-label attack step. The objective of the soft-label attack step is to modify the image to change the hash without considering the image quality constraint, whereas the objective of the hard-label attack step is to reduce adversarial image quality degradation.

Consider the original image \mathbf{I}_0 with hash value $\mathbf{h}_0 = \mathcal{H}(\mathbf{I}_0)$. The objective of the client adversary is to generate an adversarial image \mathbf{I}_{adv} with new hash $\mathbf{h}_{\text{adv}} = \mathcal{H}(\mathbf{I}_{\text{adv}})$. In an untargeted attack, \mathbf{h}_0 and \mathbf{h}_{adv} should be different enough. In a targeted attack, there is a target hash $\mathbf{h}_{\text{tar}} \neq \mathbf{h}_0$, which may be obtained from some target image as $\mathbf{h}_{\text{tar}} = \mathcal{H}(\mathbf{I}_{\text{tar}})$, and we require that \mathbf{h}_{tar} and \mathbf{h}_{adv} are similar. In both attacks, the distance between \mathbf{I}_0 and \mathbf{I}_{adv} should be small.

To simplify notation, let us use normalized Hamming distance to evaluate the similarity of two N -bit hashes as

$$D_h(\mathbf{h}_0, \mathbf{h}_{\text{adv}}) = \frac{1}{N} \sum_{n=1}^N \mathbb{I}(\mathbf{h}_0(n) = \mathbf{h}_{\text{adv}}(n)) \quad (1)$$

for two hashes with hash bits $\mathbf{h}_0(n)$ and $\mathbf{h}_{\text{adv}}(n)$, where $\mathbb{I}(x)$ is the indicator function, i.e. $\mathbb{I}(x) = 1$ if x is true and 0 otherwise. In addition, we use per-pixel normalized L_2 norm to evaluate the distance of two images, i.e.

$$L_2(\mathbf{I}_0, \mathbf{I}_{\text{adv}}) = \sqrt{\frac{1}{M} \sum_{m=1}^M (\mathbf{I}_0(m) - \mathbf{I}_{\text{adv}}(m))^2} \quad (2)$$

for two images with pixels $\mathbf{I}_0(m)$ and $\mathbf{I}_{\text{adv}}(m)$. Other measures such as SSIM are also used in our experiments.

The first step of the proposed JSHA algorithm is to apply soft-label blackbox attack to generate an initial adversarial image \mathbf{I}_{init} , with the objective to make the hash $\mathbf{h}_{\text{init}} = \mathcal{H}(\mathbf{I}_{\text{init}})$ far away from \mathbf{h}_0 for untargeted attacks or close to \mathbf{h}_{tar} for targeted attacks. This step is formulated as the optimization

$$\max_{\delta} D_h(\mathbf{h}_0, \mathcal{H}(\mathbf{I}_0 + \delta)) \quad (3)$$

in case of untargeted attacks, or

$$\min_{\delta} D_h(\mathbf{h}_{\text{tar}}, \mathcal{H}(\mathbf{I}_0 + \delta)) \quad (4)$$

in case of targeted attacks. The optimization is conducted iteratively. During each iteration, the adversary queries the PHAs with its adversarial input $\mathbf{I}_0 + \delta$ to get the hash, and uses the hash to optimize the loss (3) or (4). After reaching the query number threshold or the hash distance threshold, this first step stops with output $\mathbf{I}_{\text{init}} = \mathbf{I}_0 + \delta$.

The second step applies a hard-label blackbox attack to reduce the image distortion while maintaining the hash distance obtained in the first step. Specifically, this step solves the following optimization

$$\begin{aligned} \min_{\mathbf{I}_{\text{adv}}} L_2(\mathbf{I}_0, \mathbf{I}_{\text{adv}}), \\ \text{s.t. } D_h(\mathbf{h}_0, \mathcal{H}(\mathbf{I}_{\text{adv}})) > p \text{ (for untargeted attack)} \\ D_h(\mathbf{h}_0, \mathcal{H}(\mathbf{I}_{\text{adv}})) < p \text{ (for targeted attack)} \end{aligned} \quad (5)$$

where p is the pre-set hash distance threshold. Starting from $\mathbf{I}_{\text{adv}} = \mathbf{I}_{\text{init}}$, the adversary queries the PHAs to get the hash and uses the queried hash to optimize (5) until the pre-set maximum query number or the threshold of $L_2(\mathbf{I}_0, \mathbf{I}_{\text{adv}})$ is reached.

The proposed algorithm is outlined in Algorithm 1. One of its major advantages is query efficiency. A large learning rate can be applied in the first step to get an initial adversarial sample quickly using a small number of queries. In the second step, since we start from \mathbf{I}_{init} which is only a noisy version of \mathbf{I}_0 , the convergence is also fast. This makes our algorithm able to generate adversarial samples quickly with a very small number of queries.

2) *Robustness to Adversarial Blackbox Attacks:* Algorithm 1 and most existing blackbox attack algorithms rely on gradient estimation to solve the optimization problem. Drawing on the property of PHAs and our prior work on adversarial robust analysis [31], we have the following proposition.

Proposition 1. Gradient estimation based on queried hash is not reliable.

Algorithm 1 JSHA: Joint Soft-Label and Hard-Label Attack

- 1: **Initialization:** Original input \mathbf{I}_0 and its hash \mathbf{h}_0 ; Target hash \mathbf{h}_{tar} in case of targeted attacks.
- 2: **Step One: Unconstrained soft-label attack**
 - The adversary uses queries to optimize (3) or (4)
 - Stop and output \mathbf{I}_{init} when the pre-set hash distance threshold or query budget is reached.
- 3: **Step Two: Constrained hard-label attack**
 - The adversary uses queries to optimize (5)
 - Stop and output \mathbf{I}_{adv} when the pre-set image distortion threshold or query budget is reached.

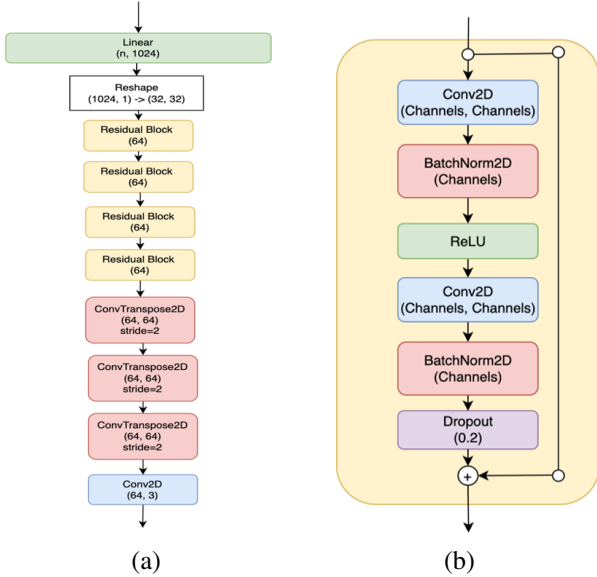


Fig. 1. (a) Hash inversion attack model. (b) Architecture of residual block.

Proof. Without loss of generality, consider the optimization problem (4). A common approach involves utilizing K randomly perturbed images to query the PHAs and then using the queried hashes to estimate the gradient as follows

$$\mathbf{g} = \frac{1}{K} \sum_{k=1}^K \frac{1}{\beta} \mathbf{u}_k D_h(\mathbf{h}_{\text{tar}}, \mathcal{H}(\mathbf{I}_0 + \delta + \beta \mathbf{u}_k)) \quad (6)$$

where $\beta \mathbf{u}_k$ represents random perturbation [19]. Firstly, due to the nature of PHAs, overly small perturbations may not induce any change in hash. Hence, relatively large β is required, but this renders the gradient estimation unreliable. Secondly, the hash $\mathcal{H}(\mathbf{I}_0 + \delta + \beta \mathbf{u}_k)$ randomly varies with the small perturbation $\beta \mathbf{u}_k$. The random variation can be modeled as a noise term Z with variance σ^2 . Following the analysis of [31], this noise is amplified by $1/\beta$, leading to the gradient estimate \mathbf{g} being affected by a noise power σ^2/β^2 , hence making it unreliable.

Due to the random nature of PHAs, it is almost impossible to limit the change of hash to just one or a few hash bits by perturbations. Practical σ is usually around 0.1. β may be around 0.001. As per [31], the signal-to-noise-ratio (SNR) of the gradient estimation can fall well below -40 dB, which makes the adversary's optimization not convergent or converge

extremely slowly. This implies that PHAs are theoretically robust to blackbox attacks under the query budget constraint.

C. Hash Inversion Attacks

GAN (generative adversarial network) was used by [12]. However, the service provider adversary may need more efficient hash inversion models because the training data may not be abundant in practice. For this, we train new and more efficient generative models to reconstruct the original input images from the hashes. We designed a decider style DNN, similar to the Fast Style Transfer [32], to convert the N -bit hashes to (64, 64) images. This DNN is mainly a combination of residual blocks, which are described in Fig. 1(b), with fractionally-strided convolutions/deconvolutions that are used for learned upsampling. The entire architecture is described in Fig. 1(a).

For a given training dataset, we first compute the hashes of each image offline and store the image-hash pairs. We then train the model outlined above to reconstruct the images as closely as possible by minimizing the mean-square-error (MSE) loss between the DNN output and the image from which the hash was generated.

IV. EXPERIMENT

A. Performance Metrics

For assessing the robustness against blackbox attacks, we employ the attack success rate as the evaluation metric. Given a set of M original images \mathbf{I}_0^m with their corresponding hashes \mathbf{h}_0^m , the adversary generates adversarial images $\mathbf{I}_{\text{adv}}^m$ along with their hashes $\mathbf{h}_{\text{adv}}^m$. The attack success rate is defined as

$$\text{ASR}(p) = \frac{1}{M} \sum_{m=1}^M \mathbb{I}(D_h(\mathbf{h}_0^m, \mathbf{h}_{\text{adv}}^m) > p) \mathbb{I}(L_2(\mathbf{I}_0^m, \mathbf{I}_{\text{adv}}^m) < \theta) \quad (7)$$

for untargeted attacks, and

$$\text{ASR}(p) = \frac{1}{M} \sum_{m=1}^M \mathbb{I}(D_h(\mathbf{h}_{\text{tar}}^m, \mathbf{h}_{\text{adv}}^m) < p) \mathbb{I}(L_2(\mathbf{I}_0^m, \mathbf{I}_{\text{adv}}^m) < \theta) \quad (8)$$

for targeted attacks (with the target hash \mathbf{h}_{tar}). $p \in [0, 1]$ is the pre-set hash distance threshold and θ is the pre-set image distortion threshold. The adversary can adjust the threshold p to control the tradeoff between the true positive rate (TPR) and the false positive rate (FPR) of the hash or image similarity decisions.

Untargeted attacks use a large p because \mathbf{h}_{adv} should be different from \mathbf{h}_0 . As shown in Fig. 2, when we calculated $D_h(\mathbf{h}_0, \mathbf{h}_1)$ of distinct images of the ImageNet validation dataset, we found that very few pairs of images had $D_h(\mathbf{h}_0, \mathbf{h}_1) < 0.3$, which was also observed in [11]. Therefore, we primarily use $p = 0.3$ in (7) to determine the success of untargeted attacks. In contrast, targeted attacks use a small p to make sure \mathbf{h}_{adv} is sufficiently close to \mathbf{h}_{tar} . Prior studies [11] indicate that many normal image edits would change an image's hashes to the level of $D_h(\mathbf{h}_0, \mathbf{h}_1) < 0.1$.

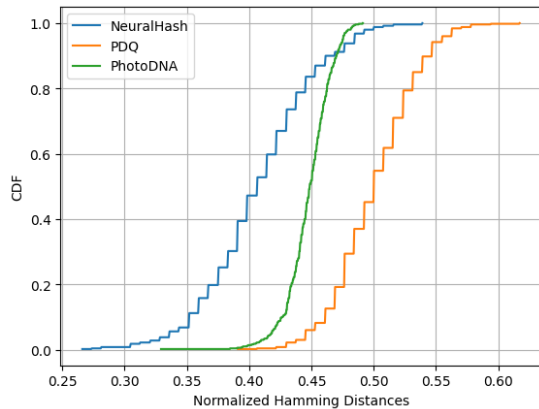


Fig. 2. Cumulative distribution function (cdf) of normalized hamming distance $D_h(\mathbf{h}_0, \mathbf{h}_1)$ between hashes of distinct images in the ImageNet validation dataset.

Therefore, we mainly use $p = 0.1$ in (8) for assessing the success of targeted attacks.

To comprehensively assess attack success, we collect $ASR(p)$ for all $p = 0.1, 0.2, 0.3, 0.4$ during experiments. We set the image distortion threshold $\theta = 0.1$.

For hash inversion attacks, we use the L_2 distortion (2), the SSIM (Structural Similarity Index Measure) [33], and the LPIPS (Learned Perceptual Image Patch Similarity) [34] between the reconstructed image and the true image to evaluate the performance. No ASR or query budget is involved.

B. Experiment Results of Image Editing Attacks

We experimented with four image editing operations that can keep the original high image quality: JPEG compression with random quality factors, resizing images with random scaling factors, filtering images with the vignette filter, or rotating images to random degrees. We calculated the hashes \mathbf{h}_0 and \mathbf{h}_1 of the images before and after the editing, and derived their distance $D_h(\mathbf{h}_0, \mathbf{h}_1)$. Using 1000 images from the ImageNet validation dataset, we obtained $ASR(p)$ for various p based on (7), wherein the L_2 condition was removed by setting θ to infinity.

Experiment results are presented in Tables I. The data for $ASR(.3)$ is highlighted in black because $p = 0.3$ is the threshold we suggested to focus on. It is evident that all three PHAs were robust to compression and resizing, but not to filtering and rotation. In conjunction with the findings in [11] [25], the PHAs are robust to many standard image editing operations except the following:

- PhotoDNA is not robust to: filtering, rotating, resizing, mirroring, bordering, cropping;
- PDQ is not robust to: filtering, rotating, mirroring [11], bordering [11], cropping [11];
- NeuralHash is not robust to: filtering, rotating, mirroring [11].

NeuralHash was the most robust among the three. Surprisingly, the newest edition of NeuralHash that we experimented with was still not robust to filtering, rotating, and mirroring, similar to the first edition experimented in [11] [25], even

TABLE I
ADVERSARY'S $ASR(p)$ WITH IMAGE EDITING ATTACKS

ASR	Compress	Resize	Filter	Rotate
PhotoDNA ASR(.1)	3%	99%	100%	100%
PhotoDNA ASR(.2)	0%	55%	100%	100%
PhotoDNA ASR(.3)	0%	0%	94%	100%
PhotoDNA ASR(.4)	0%	0%	37%	98%
PDQ ASR(.1)	0%	27%	88%	100%
PDQ ASR(.2)	0%	0%	67%	100%
PDQ ASR(.3)	0%	0%	44%	100%
PDQ ASR(.4)	0%	0%	27%	100%
NeuralHash ASR(.1)	0%	22%	96%	100%
NeuralHash ASR(.2)	0%	0%	82%	100%
NeuralHash ASR(.3)	0%	0%	57%	96%
NeuralHash ASR(.4)	0%	0%	12%	31%

though DNNs can be trained to be invariant to such standard operations with data augmentation.

C. Experiment Results of Untargeted Blackbox Attacks

In implementing our proposed JSHA algorithm, we modified three different soft-label attack algorithms: SimBA [21], NES [19], and ZOSignSGD [20], to use in Step One, and modified the hard-label attack algorithm HSJA [22] to use in Step Two. For instance, “SimBA+HSJA” means our JSHA with a modified SimBA as Step One and a modified HSJA as Step Two. Modifications included removing/changing constraints and adjusting hyper-parameters, etc. Specifically, in Step One, we skipped image distortion constraints and adopted extremely large perturbation step sizes, e.g, using a perturbation magnitude of $\epsilon = 0.9$ for SimBA instead of the original $\epsilon = 0.01$ as described in [21].

The experiments were conducted on 100 randomly selected images from the ImageNet validation dataset. Step One was executed for a total of 3000 queries unless the early stopping criterion was met. Step Two was run for an additional 2000 queries unless meeting the early stopping criterion. The main challenge for us was the CPU-based non-parallel PHA executables, which limited the number of images or queries we could process. In comparison, [28] only utilized 30 images in experiments.

Experiment results are presented in Tables II. We compared the proposed JSHA with the straightforward application of standard SimBA [21], NES [19], and ZOSignSGG [20] algorithms. We also compared it with [26] and [28].

With a focus on $ASR(0.3)$, the data indicated that NeuralHash was relatively robust because the maximum $ASR(0.3)$ was 28% only. PDQ was robust against all adversarial attacks, with a maximum $ASR(0.3)$ of 1% only. It’s worth noting that although [26] achieved a much higher attack success rate against PDQ, it required significantly more queries. It could afford millions of queries due to its access to the PDQ source code, enabling faster computation.

Furthermore, the experiment data revealed that our proposed JSHA outperformed standard blackbox attack algorithms. SimBA+HSJA surpassed [28] in attacking PhotoDNA, as the latter produced more noisy adversarial images and utilized more queries.

TABLE II
ADVERSARY'S ASR(p) WITH UNTARGETED BLACK-BOX ATTACKS.
(PH: PHOTODNA. PD: PDQ. NH: NEURALHASH.)

ASR	SimBA	SimBA +HSJA	NES	NES+ HSJA	ZO- sign- SGD	ZOsign -SGD +HSJA
PH ASR(.1)	100%	100%	18%	100%	1%	98%
PH ASR(.2)	80%	100%	2%	98%	0%	90%
PH ASR(.3)	1%	92%	0%	69%	0%	19%
PH ASR(.4)	0%	0%	0%	1%	0%	0%
PD ASR(.1)	0%	45%	0%	64%	0%	8%
PD ASR(.2)	0%	1%	0%	10%	0%	0%
PD ASR(.3)	0%	0%	0%	1%	0%	0%
PD ASR(.4)	0%	0%	0%	0%	0%	0%
NH ASR(.1)	4%	88%	0%	99%	0%	94%
NH ASR(.2)	2%	23%	0%	77%	0%	42%
NH ASR(.3)	0%	14%	0%	28%	0%	2%
NH ASR(.4)	0%	0%	0%	0%	0%	0%

[28] PH ASR(.3)= 90%, ($L_2 = 0.2$, HSJA with 3×10^4 queries)
[26] PD ASR(.3)= 73%, ($L_2 = 0.1$, up to 8×10^6 queries)

TABLE III
DISTORTION OF THE ADVERSARIAL IMAGE SAMPLES IN FIG. 3(B).

Measure	Threshold p	PhotoDNA	PDQ	NeuralHash
L_2	$p = 0.1$	0.02	0.07	0.02
	$p = 0.2$	0.02	0.11	0.04
	$p = 0.3$	0.05	0.14	0.07
	$p = 0.4$	0.17	0.19	0.19

Sample adversarial images generated with our proposed JSHA with various pre-set threshold p are depicted in Fig. 3, with their corresponding distortion metrics listed in Table III. Notably, the three images with $p = 0.4$ were deemed invalid adversarial images as their distortion was not under the threshold $\theta = 0.1$, resulting in extremely noisy images. Similarly, for PDQ, the adversarial images with $p = 0.2$ and 0.3 were also invalid.

In summary, contrary to previous studies suggesting that PHAs were not robust against untargeted attacks, we found that some PHAs like PDQ and NeuralHash could be considered as robust if realistic constraints regarding image distortion and query budget are taken into account.

D. Experiment Results of Targeted Blackbox Attacks

The experiment setting of targeted attacks was similar to that of untargeted attacks, except for utilizing \mathbf{h}_{tar} obtained from random images instead of \mathbf{h}_0 . Results are presented in Tables IV. With a focus on ASR(0.1) in this case, we observed that all targeted attacks failed, yielding $\text{ASR}(0.1) = 0$. To our knowledge, no literature has ever reported non-zero ASR(0.1), suggesting that all the PHAs are robust against targeted attacks.

The robustness is extremely strong because of $\text{ASR}(p) \approx 0$ across all p . The only exception was NeuralHash, which exhibited ASR(0.4) of 43% with SimBA. However, this isn't indicative of successful adversarial attacks; rather, it's due to numerous hashes generated by NeuralHash having $D_h(\mathbf{h}_0, \mathbf{h}_1)$ as low as 0.3, as illustrated in Fig. 2. Under NeuralHash, many images are inherently adversarial when evaluated at $p = 0.4$.

In summary, contrary to the prior claims that PHAs were not robust against targeted attacks [28], our findings demonstrate



Fig. 3. Samples of an original image and the adversarial images created by the proposed untargeted blackbox attack algorithm JSHA (NES+HSJA).

the strong robustness of all PHAs against targeted blackbox attacks. This is significant to the practical application of PHAs because the client adversary needs targeted attacks to ensure that its adversarial hashes do not inadvertently match illicit hashes in the database. The strong robustness means it is hard for the adversary to undertake either untargeted or targeted attacks without being caught.

E. Experiment Results of Hash Inversion Attacks

To demonstrate the service provider adversary's capability to reconstruct original images from their hashes under some contextual knowledge, such as the group of images to which

TABLE IV
ADVERSARY'S ASR(p) WITH TARGETED BLACKBOX ATTACKS.
(PH: PHOTODNA. PD: PDQ. NH: NEURALHASH)

ASR	SimBA	SimBA +HSJA	NES	NES+ HSJA	ZO- sign- SGD	ZOsign -SGD +HSJA
PH ASR(.1)	0%	0%	0%	0%	0%	0%
PH ASR(.2)	0%	0%	0%	0%	0%	0%
PH ASR(.3)	0%	0%	0%	0%	0%	0%
PH ASR(.4)	1%	2%	0%	0%	0%	0%
PD ASR(.1)	0%	0%	0%	0%	0%	0%
PD ASR(.2)	0%	0%	0%	0%	0%	0%
PD ASR(.3)	0%	0%	0%	0%	0%	0%
PD ASR(.4)	0%	0%	0%	0%	0%	0%
NH ASR(.1)	0%	0%	0%	0%	0%	0%
NH ASR(.2)	0%	0%	0%	0%	0%	0%
NH ASR(.3)	0%	0%	0%	0%	0%	0%
NH ASR(.4)	43%	11%	0%	0%	0%	0%
[28] PH ASR(.3) ($L_2 = 0.19$)			83%	$(2 \times 10^6$ queries)		
[28] PD ASR(.3) ($L_2 = 0.42$)			100%	$(6 \times 10^5$ queries)		

TABLE V
QUALITY OF ADVERSARIAL IMAGES CREATED IN HASH INVERSION
ATTACKS (PH: PHOTODNA. PD: PDQ. NH: NEURALHASH)

Dataset	Hash	L_2	SSIM	LPIPS
MNIST	PH	0.08 \pm 0.02	0.79 \pm 0.02	0.18 \pm 0.03
	PD	-	-	-
	NH	0.19 \pm 0.05	0.35 \pm 0.10	0.33 \pm 0.08
CelebA	PH	0.13 \pm 0.03	0.57 \pm 0.08	0.40 \pm 0.07
	PD	0.23 \pm 0.07	0.44 \pm 0.07	0.43 \pm 0.05
	NH	0.23 \pm 0.05	0.29 \pm 0.09	0.53 \pm 0.07

the original images may belong, we conducted experiments using two datasets MNIST and CelebA as known contexts. For each hashing algorithm and dataset, we trained the inversion network depicted in Fig. 1 for 50 epochs, with a batch size of 64 and an initial learning rate of 0.005. We utilized the MSE loss function with the AdamW optimizer and the cosine annealing learning rate scheduler.

Results are presented in Table V. Samples of synthesized images along with their original images can be observed in Fig. 4 and Fig. 5. It is evident that the hash leaks sufficient information for image reconstruction when certain contextual information is known, such as whether the image belongs to MNIST digits or CelebA photos. Although no image quality metrics were given in [12], Fig. 5(c) shows that our proposed model had a performance comparable to that of [12].

In Table V, smaller L_2 and LPIPS mean better image reconstruction, while larger SSIM means better image reconstruction. PhotoDNA has the longest hashes at 1152-bits, PDQ has 256-bit hashes and NeuralHash has 96-bit hashes. Intuitively, this implies that PhotoDNA hashes contain the most information about the original images while NeuralHash hashes contain the least. Table V supported this intuition.

The results in the MNIST for PDQ were left blank because PDQ could not work on MNIST. PDQ outputs quality scores of 0 for every image, and each of the hash values calculated turned out to be a 256-dimensional vector of zeros for MNIST images.

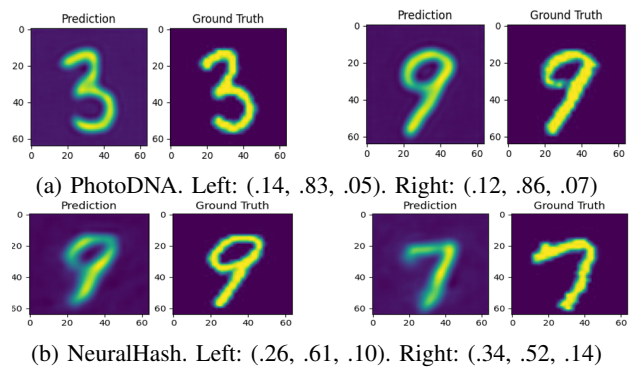


Fig. 4. Samples of true images and adversarial images generated by hash inversion attacks based on hashes of (a) PhotoDNA, and (b) NeuralHash. The numbers are (L_2 , SSIM, LPIPS) measures.

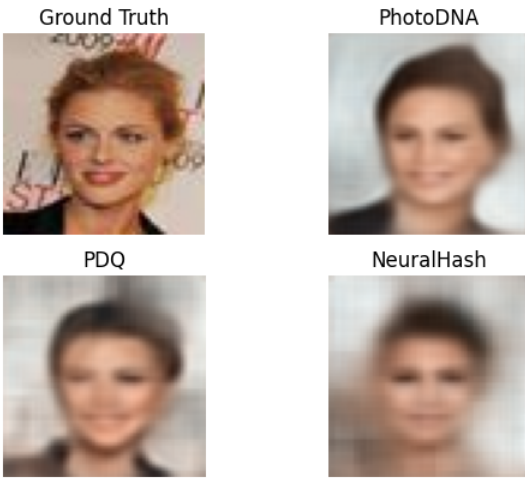
V. CONCLUSIONS

This paper presents a thorough examination of the security of three real-world perceptual hashing algorithms (PHAs): PhotoDNA, PDQ, and NeuralHash, against three distinct types of attacks: standard image editing attacks, malicious adversarial blackbox attacks, and hash inversion attacks. To support the security study, a query-efficient blackbox adversarial attack algorithm named Joint Soft-label and Hard-label Attack (JSHA) is designed to expedite blackbox adversarial attacks while requiring fewer queries. Additionally, the paper proposes a new data-efficient hash inversion network capable of reliably reconstructing original images from all hashes, even those of very short length.

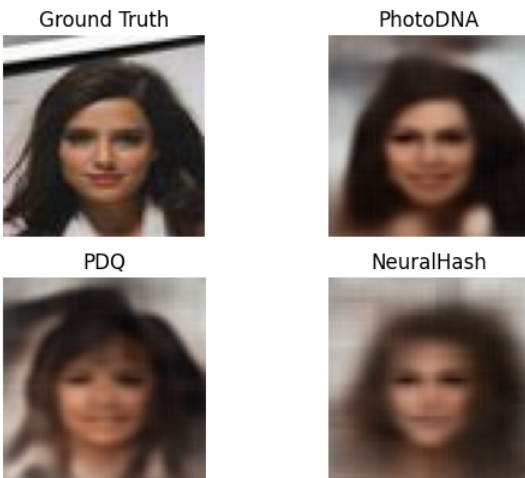
The findings of the study indicate that PHAs exhibit robustness against blackbox adversarial attacks when realistic constraints regarding adversarial image distortion and query budget are taken into consideration. However, the vulnerabilities to certain image editing methods and the potential information leakage through the hashes raise significant security concerns. These insights underscore the importance of further research and development efforts to enhance the resilience and security of perceptual hashing algorithms in practical applications.

REFERENCES

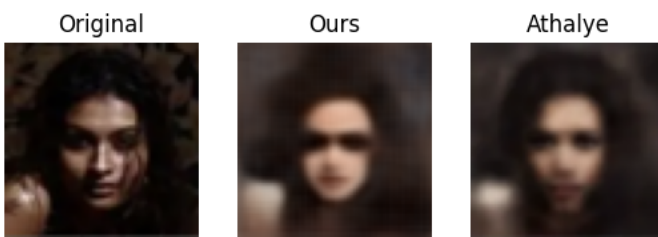
- [1] Mauro Barni, Patrizio Campisi, Edward J Delp, Gwenaël Doërr, Jessica Fridrich, Nasir Memon, Fernando Pérez-González, Anderson Rocha, Luisa Verdoliva, and Min Wu, "Information forensics and security: A quarter-century-long journey," *IEEE Signal Processing Magazine*, vol. 40, no. 5, pp. 67–79, 2023.
- [2] Hany Farid, "An overview of perceptual hashing," *Journal of Online Trust and Safety*, vol. 1, no. 1, 2021.
- [3] Sivic and Zisserman, "Video google: A text retrieval approach to object matching in videos," in *Proceedings ninth IEEE international conference on computer vision*. IEEE, 2003, pp. 1470–1477.
- [4] Qingying Hao, Licheng Luo, Steve TK Jan, and Gang Wang, "It's not what it looks like: Manipulating perceptual hashing based applications," in *Proceedings of the 2021 ACM SIGSAC Conference on Computer and Communications Security*, 2021, pp. 69–85.
- [5] Wayne A Logan, "Citizen searches and the duty to report," *Ohio St. LJ*, vol. 83, pp. 939, 2022.
- [6] Tracy Ith, "Microsoft's photodna: Protecting children and businesses in the cloud," Retrieved from Microsoft News Center: <https://news.microsoft.com/features/microsofts-photodna-protecting-children-and-businesses-in-the-cloud>, 2015.
- [7] Antigone Davis and Guy Rosen, "Open-sourcing photo-and video-matching technology to make the internet safer," *Facebook Newsroom*, 2019.



(a) Our model. $\{L_2, SSIM, LPIPS\} = \{.14, .65, .34\}$ (PhotoDNA), $= \{.15, .60, .36\}$ (PDQ), $\{.20, .40, .50\}$ (NeuralHash)



(b) Our model. $\{L_2, SSIM, LPIPS\} = \{.17, .63, .34\}$ (PhotoDNA), $= \{.21, .50, .34\}$ (PDQ), $\{.20, .47, .45\}$ (NeuralHash)



(c) Compare images generated by our model and [12].

Fig. 5. Samples of true images and reconstructed images generated by hash inversion attacks from hashes of PhotoDNA, PDQ, and NeuralHash. The numbers are quality metrics $\{L_2, SSIM, LPIPS\}$ of reconstructed images.

[8] Anunay Kulshrestha and Jonathan Mayer, "Identifying harmful media in {End-to-End} encrypted communication: Efficient private membership computation," in *30th USENIX Security Symposium (USENIX Security 21)*, 2021, pp. 893–910.

[9] Jennifer Cobbe, "Data protection, eprivacy, and the prospects for apple's on-device csam detection system in europe," *SocArXiv*, 2021.

[10] Harold Abelson, Ross Anderson, Steven M Bellovin, Josh Benaloh, Matt Blaze, Jon Callas, Whitfield Diffie, Susan Landau, Peter G Neumann, Ronald L Rivest, et al., "Bugs in our pockets: The risks of client-side scanning," *Journal of Cybersecurity*, vol. 10, no. 1, pp. tyad020, 2024.

[11] Sean McKeown and William J Buchanan, "Hamming distributions of

popular perceptual hashing techniques," *Forensic Science International: Digital Investigation*, vol. 44, pp. 301509, 2023.

[12] Anish Athalye, "Inverting photodna," <https://anishathalye.com/inverting-photodna/>, 2021.

[13] Gannon Burgett, "Photodna lets google, fb and others hunt down child pornography without looking at your photos," *PetaPixel*, August, 2014.

[14] Charles Arthur, "Twitter to introduce photodna system to block child abuse images," *The Guardian*, vol. 22, 2013.

[15] Evan Klinger and David Starkweather, "phash: The open source perceptual hash library," 2013.

[16] Christian Szegedy, Wojciech Zaremba, Ilya Sutskever, Joan Bruna, Dumitru Erhan, Ian Goodfellow, and Rob Fergus, "Intriguing properties of neural networks," *arXiv preprint arXiv:1312.6199*, 2013.

[17] Aleksander Madry, Aleksandar Makelov, Ludwig Schmidt, Dimitris Tsipras, and Adrian Vladu, "Towards deep learning models resistant to adversarial attacks," *arXiv preprint arXiv:1706.06083*, 2017.

[18] Nicholas Carlini and David Wagner, "Towards evaluating the robustness of neural networks," in *2017 IEEE Symposium on Security and Privacy (SP)*. Ieee, 2017, pp. 39–57.

[19] Andrew Ilyas, Logan Engstrom, Anish Athalye, and Jessy Lin, "Black-box adversarial attacks with limited queries and information," in *International conference on machine learning*. PMLR, 2018, pp. 2137–2146.

[20] Sijia Liu, Pin-Yu Chen, Xiangyi Chen, and Mingyi Hong, "signsgd via zeroth-order oracle," in *International Conference on Learning Representations*, 2018.

[21] Chuan Guo, Jacob Gardner, Yurong You, Andrew Gordon Wilson, and Kilian Weinberger, "Simple black-box adversarial attacks," in *International Conference on Machine Learning*. PMLR, 2019, pp. 2484–2493.

[22] Jianbo Chen, Michael I Jordan, and Martin J Wainwright, "Hop-skipjumpattack: A query-efficient decision-based attack," in *2020 IEEE Symposium on Security and Privacy (SP)*. IEEE, 2020, pp. 1277–1294.

[23] Brian Dolhansky and Cristian Canton Ferrer, "Adversarial collision attacks on image hashing functions," *arXiv preprint arXiv:2011.09473*, 2020.

[24] Martin Steinebach, "An analysis of photodna," in *Proceedings of the 18th International Conference on Availability, Reliability and Security*, 2023, pp. 1–8.

[25] Lukas Struppek, Dominik Hintersdorf, Daniel Neider, and Kristian Kersting, "Learning to break deep perceptual hashing: The use case neuralhash," in *Proceedings of the 2022 ACM Conference on Fairness, Accountability, and Transparency*, 2022, pp. 58–69.

[26] Shubham Jain, Ana-Maria Crețu, and Yves-Alexandre de Montjoye, "Adversarial detection avoidance attacks: Evaluating the robustness of perceptual hashing-based client-side scanning," in *31st USENIX Security Symposium (USENIX Security 22)*, 2022, pp. 2317–2334.

[27] Jagdeep Singh Bhatia and Kevin Meng, "Exploiting and defending against the approximate linearity of apple's neuralhash," *arXiv preprint arXiv:2207.14258*, 2022.

[28] Jonathan Prokos, Neil Fendley, Matthew Green, Roei Schuster, Eran Tromer, Tushar Jois, and Yinzhi Cao, "Squint hard enough: attacking perceptual hashing with adversarial machine learning," in *32nd USENIX Security Symposium (USENIX Security 23)*, 2023, pp. 211–228.

[29] Robert Grimm, "Putting the count back into accountability: An audit of social media transparency disclosures, focusing on sexual exploitation of minors," *arXiv preprint arXiv:2402.14625*, 2024.

[30] Muhammad Shahroz Nadeem, Virginia NL Franqueira, and Xiaojun Zhai, "Privacy verification of photodna based on machine learning," in ., 93y42, 2019.

[31] Manjushree B Aithal and Xiaohua Li, "Mitigating black-box adversarial attacks via output noise perturbation," *IEEE Access*, vol. 10, pp. 12395–12411, 2022.

[32] Justin Johnson, Alexandre Alahi, and Li Fei-Fei, "Perceptual losses for real-time style transfer and super-resolution," in *Computer Vision—ECCV 2016: 14th European Conference, Amsterdam, The Netherlands, October 11–14, 2016, Proceedings, Part II 14*. Springer, 2016, pp. 694–711.

[33] Alain Hore and Djemel Ziou, "Image quality metrics: Psnr vs. ssim," in *2010 20th international conference on pattern recognition*. IEEE, 2010, pp. 2366–2369.

[34] Richard Zhang, Phillip Isola, Alexei A Efros, Eli Shechtman, and Oliver Wang, "The unreasonable effectiveness of deep features as a perceptual metric," in *Proceedings of the IEEE conference on computer vision and pattern recognition*, 2018, pp. 586–595.